Extended Abstracts of the 2018 International Conference on Solid State Devices and Materials, Tokyo, 2018, pp1139-1140

Electroluminescence from InP-based Heterostructure Nanowires

Junichi Motohisa, Hiroki Kameda, Masahiro Sasaki, and Katsuhiro Tomioka

Hokkaido University
North 14 West 9, Sapporo 060-0814, Japan
Phone: +81-11-706-6508 E-mail: motohisa@ist.hokudai.ac.jp

Abstract

We have fabricated light-emitting diodes (LEDs) using InP/InAsP/InP heterostructure nanowires (NWs). The NWs containing heterostructure and a p-i-n junction were grown by using selective-area metalorganic vapor-phase epitaxy. Electroluminescence was observed in near infrared regions at room temperature and emission from InAsP layer embedded in InP NWs was clearly shown based on a comparison of its photoluminescence spectrum.

1. Introduction

InP-based nanowires (NWs) are attractive for the application of various kinds of photonic devices, such as light-emitting diodes (LEDs)[1-3], lasers [4] and solar cells [5]. One of the important field of application is on-demand single photon sources for quantum telecommunication, and we have demonstrated InP-based NW light-emitting diodes (LEDs) [2] and emission up to S-bands by optical pumping from InAsP quantum dots (QDs) embedded in InP NWs [6]. Here we report on the electroluminescence of axial InAsP/InP heterostructure NWs at room temperature.

2. Experimental procedure

The samples were grown by SA-MOVPE [7] on a p-type InP (111) substrates partially covered with a SiO_2 mask. The mask pattern for selective-area growth consisted of array of holes with diameter d_0 ranging from 50 to 300 nm, and pitch a of 400 nm to 3 µm, and the patterns were defined within 100 µm by 100 µm regions, and this corresponded to the size of LEDs for individual NW array. Trimethylindium (TMIn), tertiarybutylphosphine (TBP), and AsH_3 were used as source materials. We first grew p-InP at 660°C with V/III ratio of 20 using diethylzinc (DEZn) as a dopant gas. This growth condition is expected to yield wurzite (WZ) InP NWs without doping [7], but Zn-doping results in the formation of zincblende (ZB) crystal with rotational twinning, or the mixing of crystal structures, as reported by Ikejiri *et al*. [8]. After the growth of undoped InP, the temperature was lowered to 580 °C and undoped InP, InAsP and InP were grown for 2 min, 3 sec, and 2 min, respectively. The supply ratio of TBP for InAsP layer, which is defined by the partial pressure of TBP over the partial pressure of sum of group V sources (namely, [TBP]/([TBP]+[AsH_3]) was 0.96, but P composition in the solid phase is much smaller than this value [6,9]. Finally, n-doped InP were grown at 660 °C using SiH_4 for a dopant source. The doping density was estimated to be 7.0×10^{17} and 3.8×10^{18} cm^{-3}, for n- and p-InP, respectively. Figure 1 shows an SEM image of the grown InP/InAsP NW array with p-i-n structure. The pitch a of the array was 1 µm. The thickness of the NWs became larger from the middle of the NWs. This is similar to our previous undoped heterostructure NWs [6,9] and we believe this demonstrated the formation of InAsP layer at the middle of the NWs. The average size of these particular NWs measured 276 nm in diameter d at top and 2.23 µm in height h.

After the NW growth, LEDs were fabricated following the procedure reported earlier [2]. The device was diced and mounted on a chip carrier and Au wire was bonded onto some of the top contact of NW-LEDs using epoxy die bonder. The measurement was carried out at room temperature and emission was observed through a ×5 microscope objective with N.A. of 0.14.

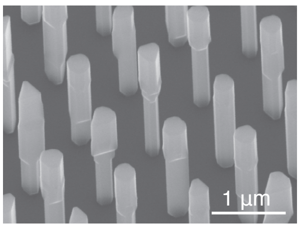

Fig. 1 SEM image of a typical grown p-i-n InP/InAsP/InP nanowire array.

3. Results and Discussions

Figure 2(a) shows typical *I-V* characteristics of fabricated NW-LEDs. The actual height and diameter was not measured for this particular device, but they were inferred to be 330 nm in diameter and 1 µm in height based on the mask pattern size dependence of NW size. The pitch of NWs was 800nm. Good rectifying characteristics were confirmed. The current I in the forward bias is about three orders of magnitude smaller than our recent homostructure InP NW-LEDs [10], while I in the reversed bias was nearly the same. Ideality factor n of the diode was roughly estimated to be about 5, as shown in the

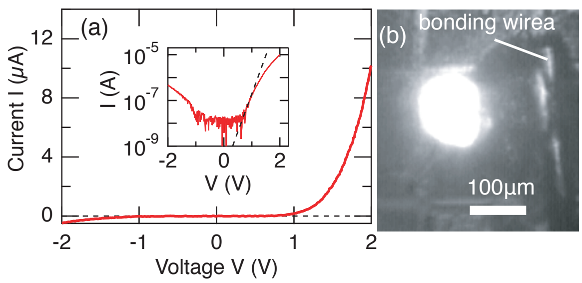

Fig. 2 *I-V* characteristics of an LED (a) and emission image at forward bias 2V.

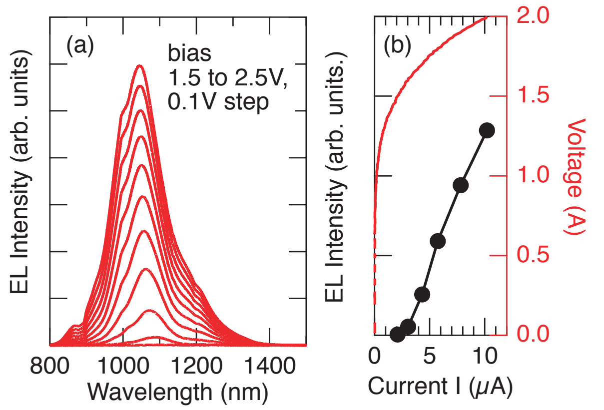

Fig. 3 Electroluminescence spectra of a NW-LED (a) and its *I*-*L* characteristics.

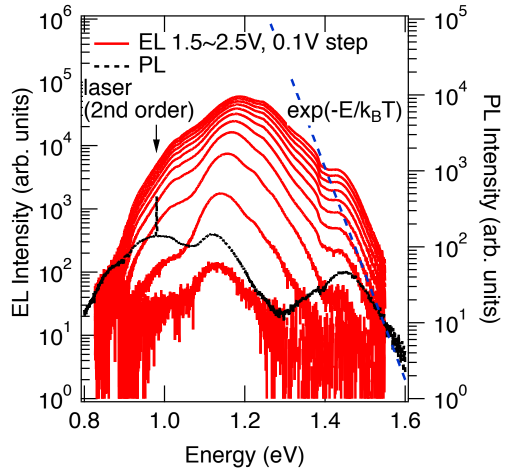

Fig. 4 Replot of Fig. 3(a) in logarithmic plot, together with PL spectrum measured at room temperature.

dashed line in the inset. This value is much larger than our recent InP NW-LEDs [10], which is slightly below 2. In addition, series resistance R_s was estimated to be 15 kΩ, and was considerably larger than InP NW-LEDs. Reasons for bad n and R_s are not clear at present and improvement is required to achieve good injection efficiency. The emission image of the LED is shown in Fig. 2(b). Considering that the sensitivity of the standard CCD camera is very low above 1000 nm, emission was thought to be reasonably bright.

Figure 3(a) shows electroluminescence (EL) spectra of the NW-LED. Broad band emission was observed in the near infrared region. The emission of the main peak was at around 1043 nm, with width of about 154 nm. Comparison with the photoluminescence (PL) peak confirmed that it was originated from an InAsP layer embedded in InP NWs, as elaborated below. We also can see that the position of the main peak shows slight blueshift with increasing injection current, which will also be discussed later. Figure 3(c) shows *I*-*L* characteristics of the device. A large offset current (about 3 μA) was observed before obtaining emission. Possible reasons for this offset could be shunting resistance or insufficient injection of carriers into InAsP from InP, but the detail is not clear at present. Nevertheless, the linearity above 3 μA was clearly better than homostructure LEDs [2,10]. This is thought to indicate that InAsP was buried in InP and nonradiative recombination, which occurs predominantly on the bare surface of InP NW, is suppressed.

Figure 4 is a replot of Fig. 3(a) in a logarithmic scale, plotted as a function of photon energy. The PL spectrum from the same sample under He-Ne excitation is also shown in the figure. Three major peaks are noticeable in PL spectrum. It should be noted that all the peak positions in the PL spectrum coincides with the peaks or peak shoulders of EL in the low injection limit. We have already reported a systematic study that the PL above 900nm originates from InAsP layers in InP NWs. Thus, the EL observed in the present study is also from InAsP layers in InP NWs. We are expecting that InAsP/InP forms a quantum well, so, the two PL peaks at around 1.12 eV (~1100 nm) and 0.98 eV (~1270 nm) is believed to be from InAsP QWs with different well width. The peak at around 1.44 eV (860 nm) is thought to originate from the WZ section of InP NWs both in the PL and EL spectra, and similar to our previous study, peak shift was not observed in EL spectra at room temperature.

Acknowledgements

The work is partially financially supported by Grant-in-aid for scientific research supported by Japan Society for Promotion of Science.

References

[1] E. D. Minot, F. Kelkensberg, M. van Kouwen, J. A. van Dam, L. P. Kouwenhoven, V. Zwiller, M. T. Borgström, O. Wunnicke, M. A. Verheijen, and E. P. A. M. Bakkers, Nano Lett. **7**, 367 (2007).

[2] S. Maeda, K. Tomioka, S. Hara, and J. Motohisa, Jpn. J. Appl. Phys. **51**, 02BN03 (2012).

[3] A. Berg, S. Yazdi, A. Nowzari, K. Storm, V. Jain, N. Vainorius, L. Samuelson, J. B. Wagner, and M. T. Borgström, Nano Lett. **16**, 656 (2016).

[4] Q. Gao, D. Saxena, F. Wang, L. Fu, S Mokkapati, Y. Guo, L. Li, J. Wong-Leung, P. Caroff, H. H. Tan, and C. Jagadish, Nano Lett. **14**, 5206 (2014).

[5] J. Wallentin, N. Anttu, D. Asoli, M. Huffman, I. Åberg, M. H. Magnusson, G. Siefer, P. Fuss-Kailuweit, F. Dimroth, B. Witzigmann, H. W. Xu, L. Samuelson, K. Deppert, M. T. Borgström, Science **339**, 1057 (2013).

[6] M. Sasaki, H. Kameda, K. Tomioka, J. Motohisa, The 24th Congress of the International Commission for Optics (ICO-24), Tokyo, Japan (2017).

[7] Y. Kitauchi, Y. Kobayashi, K. Tomioka, S. Hara, K. Hiruma, T. Fukui and J. Motohisa, Nano Lett. **10**, 1699 (2010).

[8] K. Ikejiri, F. Ishizaka, K. Tomioka, and T. Fukui, Nano Lett. **12**, 4770 (2012).

[9] Y. Kobayashi, J. Motohisa, K. Tomioka, S. Hara, K. Hiruma, and T. Fukui, Proc. Int. Conf. Indium Phosphide and Related Materials (IPRM 2010), 2010, p.1.

[10] J. Motohisa, H. Kameda, M.Sasaki, and K. Tomioka, 19th International Conference on Metalorganic Vapor Phase Epitaxy (IC-MOVPE 19), Nara, Japan (2018).